Annali dell'Università di Ferrara manuscript No.
(will be inserted by the editor)

Gašper Jaklič · Emil Žagar

Shape preserving interpolation by cubic G^1 splines in $\mathbb{R}^3$

Received: date / Accepted: date

Abstract In this paper, G^1 continuous cubic spline interpolation of data points in $\mathbb{R}^3$, based on a discrete approximation of the strain energy, is studied. Simple geometric conditions on data are presented that guarantee the existence of the interpolant. The interpolating spline is regular, loop-, cusp- and fold-free.

Keywords Hermite interpolation · Geometric continuity · Spline · Minimization

Mathematics Subject Classification (2000) 65D17 · 65D07 · 41A05

1 Introduction

The problem of a construction of an interpolating curve through a sequence of data points is one of the basic problems of CAGD (Computer Aided Geometric Design) and frequently arises in research and in practical applications, such as modeling, design,...

A great deal of research on this topic has been done (see [5] and references therein), especially on the shape preserving interpolation, since an important goal for the interpolant is to follow the data as close as possible. Many interpolation schemes exist with different resulting interpolants. For example, it

G. Jaklič
FMF, University of Ljubljana and PINT, University of Primorska, Slovenia
Tel.: +386-1-4766500
Fax: +386-1-2517281
E-mail: Gasper.Jaklic@fmf.uni-lj.si

E. Žagar
FMF and IMFM, University of Ljubljana
Tel.: +386-1-4766500
Fax: +386-1-2517281
E-mail: Emil.Zagar@fmf.uni-lj.si

is well-known, that the cubic C^2 interpolating spline minimizes the (approximate) strain energy, and thus gives a good (physically based) approximation of the data points. Unfortunately, its construction involves solving a large global system of equations, that depends on the chosen parameterization of the curve.

Beside classical approaches, in recent years a notable improvement on interpolatory subdivision schemes and geometric interpolation was made (see [4], [3], [6], [7], [9] and references therein). Here the problems are usually nonlinear and much harder to tackle than in classical approaches.

There are several goals in interpolation scheme construction. The interpolating spline should be regular and without unwanted behaviour, such as loops, cusps or folds on spline segments. Furthermore, it should closely follow the data polygon (the polygon, defined by the sequence of data points) and be pleasing to the human eye - a condition, which is quite difficult to express in mathematical terms.

The scheme should be local if possible, since thus an efficient construction of the spline can be done, and solving of a large global system of equations can be avoided.

Usually, the Lagrange interpolation does not have enough shape parameters to sufficiently control the shape of the curve. The Hermite interpolation adds the choice of tangent directions. They can be given as prescribed data, be locally constructed or manipulated by the designer, or be automatically generated in some intelligent way. If the first possibility is given, then the cubic Hermite interpolation problem always has a unique solution. Practical examples have shown, that the tangent directions, interactively given by the designer, can quickly give curves with unwanted behaviour. This approach is thus useful in practice just for small local corrections of the shape of the curve. The last possibility is the most complicated, since the scheme should guarantee the existence of the interpolant and furthermore, construct tangent directions in an appropriate way.

In this paper, we will focus on the third possibility, a local scheme for the construction of the interpolating spline through the given data points in $\mathbb{R}^3$. Simple geometric conditions on tangent directions will be given, that guarantee the existence of the interpolant. A heuristic for automatic generation of admissible tangent directions, based on the analysis of the planar case ([8]) will be used for the construction of the spline interpolant. The resulting interpolant closely resembles the cubic C^2 interpolating spline, which minimizes the (approximate) strain energy of the curve.

The paper is organized as follows. In Section 2 the interpolation problem is presented and the strain energy is recalled. In Section 3 the discrete approximation of the (approximate) strain energy is derived, and the shape of the interpolating spline is analyzed. The paper is concluded by some examples in Section 4.

2 Interpolation problem and the strain energy

The problem considered is as follows. Suppose that we are given data points

$$\boldsymbol{T}_j \in \mathbb{R}^3, \quad \boldsymbol{T}_j \neq \boldsymbol{T}_{j+1}, \quad j = 0, 1, \ldots, n,$$

and associated interpolation parameters

$$t_j \in \mathbb{R}, \quad j = 0, 1, \ldots, n, \quad t_0 < t_1 < \cdots < t_n. \tag{1}$$

Usually the interpolation parameters are derived from the data points by the centripetal or the chord length parameterization (or by some other method), but in general we will assume that they are prescribed in advance. Our goal is to find a G^1 continuous parametric spline curve $\boldsymbol{s} : [t_0, t_n] \to \mathbb{R}^3$ such that

$$\begin{aligned}
&\boldsymbol{s}_i := \boldsymbol{s}|_{[t_{i-1}, t_i]} \in \mathbb{P}_3, \quad i = 1, 2, \ldots, n, \\
&\boldsymbol{s}_i(t_k) = \boldsymbol{T}_k, \quad k = i-1, i, \quad i = 1, 2, \ldots, n, \\
&\boldsymbol{s}_i'(t_k) = \alpha_{i,k-i+1}\, \boldsymbol{d}_k, \quad k = i-1, i, \quad i = 1, 2, \ldots, n,
\end{aligned} \tag{2}$$

where $\alpha_{i,k-i+1} > 0$ are unknown positive scalars, $\boldsymbol{d}_k$ normalized tangent direction vectors, and $\mathbb{P}_3$ is the space of parametric polynomials of degree ≤ 3. There are infinitely many solutions of this problem, since it is well-known that any set of $\alpha_{i,k-i+1} > 0$ and $\boldsymbol{d}_k$ gives a unique spline curve $\boldsymbol{s}$. Thus a large set of free parameters is available that can be used to design an appropriate shape of the interpolatory curve.

One of the natural approaches how to deal with the free parameters is to define a suitable functional and minimize it. Usually, the shape of the curve depends mostly on its curvature κ and therefore it seems reasonable to minimize the functional

$$\varphi_s(\boldsymbol{\alpha}) := \int_{t_0}^{t_n} \|\kappa(t)\|^2 \, dt = \int_{t_0}^{t_n} \frac{\|\boldsymbol{s}'(t) \times \boldsymbol{s}''(t)\|^2}{\|\boldsymbol{s}'(t)\|^6} \, dt, \tag{3}$$

where $\boldsymbol{\alpha} := (\alpha_{i,k-i+1})_{i=1,k=i-1}^{n,i} \in \mathbb{R}^{2n}$. The expression (3) is called **the strain energy** of the curve. In practice ([2], [10]), the approximate strain energy (called also **linearized bending energy**)

$$\varphi(\boldsymbol{\alpha}) := \int_{t_0}^{t_n} \|\boldsymbol{s}''(t)\|^2 \, dt, \tag{4}$$

is used instead of (3). Note that the approximate strain energy is close to a real one if $\|\boldsymbol{s}'(t)\| \approx 1$. If this is not the case, it can be far away from the real strain energy. But the beauty of the approximant lies in the fact that the minimization problem for the coefficients becomes linear.

Note also that in our case the curve $\boldsymbol{s}$ is only G^1, thus $\boldsymbol{s}''$ might not be continuous, but since it has only a finite number of finite jumps, the integral (4) clearly exists.

The approach of minimizing (4) has been used in the paper [11]. There the authors assumed that the tangent directions are given in advance. It turned out that some unwanted situations occur that have to be solved by adding artificial data. This can be quite computationally intensive when dealing with a huge number of data.

In this paper we will consider a similar approach, that will resolve the above mentioned problems. Instead of minimizing the approximate strain energy (4), we will minimize its discrete approximation. Of course, the positivity of scalar parameters $\alpha_{i,k-i+1}$ must be taken into account, which obviously leads to a constrained optimization problem. On the contrast to [11] where tangent directions were given in advance, we will only need the data points, and shall consider that the tangent directions are determined in some feasible way. One of the possible approaches how to choose tangent directions will be described.

3 Analysis of the interpolating spline

Let us introduce the notation used in the paper. Let $\langle\cdot,\cdot\rangle$ be the standard inner product in $\mathbb{R}^3$ and $\angle(\boldsymbol{a},\boldsymbol{b})$ the angle formed by the vectors $\boldsymbol{a}$ and $\boldsymbol{b}$. Recall that

$$\langle\boldsymbol{a},\boldsymbol{b}\rangle = \|\boldsymbol{a}\|\,\|\boldsymbol{b}\|\,\cos\angle(\boldsymbol{a},\boldsymbol{b}).$$

We will use the standard forward difference notation, $\Delta(\bullet)_i = (\bullet)_{i+1} - (\bullet)_i$, and a divided difference

$$[u_i, u_{i+1}, \ldots, u_{k-1}, u_k]f = \frac{[u_{i+1}, \ldots, u_k]f - [u_i, \ldots, u_{k-1}]f}{u_k - u_i},$$

with $[u_i]f = f(u_i)$ and $[\underbrace{u_i, \ldots, u_i}_{j}]f = \frac{f^{(j-1)}(u_i)}{(j-1)!}$.

Consider the (approximate) strain energy functional φ in (4). If

$$\varphi_i(\boldsymbol{\alpha}) := \int_{t_{i-1}}^{t_i} \|\boldsymbol{s}_i''(t)\|^2\,dt, \quad i = 1, 2, \ldots, n,$$

then φ can be written as

$$\varphi(\boldsymbol{\alpha}) = \sum_{i=1}^{n} \varphi_i(\boldsymbol{\alpha}).$$

We want to minimize it on the open set $\mathcal{D} = \{\boldsymbol{\alpha} \in \mathbb{R}^{2n} \,|\, \boldsymbol{\alpha} > \boldsymbol{0}\}$. Here the inequality $\boldsymbol{\alpha} > \boldsymbol{0}$ is considered componentwise. But φ_i depends only on the local parameters $\boldsymbol{\alpha}_i := (\alpha_{i,0}, \alpha_{i,1})$, thus $\varphi_i(\boldsymbol{\alpha}) = \varphi_i(\boldsymbol{\alpha}_i)$ and obviously

$$\min_{\boldsymbol{\alpha}\in\mathcal{D}} \varphi(\boldsymbol{\alpha}) = \sum_{i=1}^{n} \min_{\boldsymbol{\alpha}_i\in\mathcal{D}_i} \varphi_i(\boldsymbol{\alpha}_i),$$

where $\mathcal{D}_i = \{\boldsymbol{\alpha}_i \in \mathbb{R}^2 \,|\, \boldsymbol{\alpha}_i > \boldsymbol{0}\}$. Instead of explicitly deriving $\boldsymbol{s}_i''$ and applying minimization as in [11], a discrete approximation of φ_i will be used. This will exclude some unwanted possibilities which imply preprocessing of data points to guarantee that the minimum occurs in a desired region (for example of this, see [11], e.g.). For a large number of data points the computational cost of this can be substantial. It is clear that $\varphi_i \equiv 0$ if $\boldsymbol{s}_i$ is a line segment joining $\boldsymbol{T}_{i-1}$ and $\boldsymbol{T}_i$. In general, $\boldsymbol{s}_i$ will be a cubic polynomial of course, but a choice of an appropriate $\boldsymbol{\alpha}_i$ might minimize its first two leading coefficients and thus make it closer to its data polygon (the line $\boldsymbol{T}_{i-1}\boldsymbol{T}_i$). To find a suitable discrete approximation of φ_i, $\boldsymbol{s}_i$ will be written in the Newton form

$$\begin{aligned}\boldsymbol{s}_i(t) = \boldsymbol{T}_{i-1} &+ (t-t_{i-1})\,[t_{i-1},t_{i-1}]\boldsymbol{s}_i + (t-t_{i-1})^2\,[t_{i-1},t_{i-1},t_i]\boldsymbol{s}_i \\ &+ (t-t_{i-1})^2\,(t-t_i)[t_{i-1},t_{i-1},t_i,t_i]\boldsymbol{s}_i,\end{aligned} \tag{5}$$

where $[t_{i-1},t_{i-1}]\boldsymbol{s}_i = \alpha_{i,0}\,\boldsymbol{d}_{i-1}$ and $[t_i,t_i]\boldsymbol{s}_i = \alpha_{i,1}\,\boldsymbol{d}_i$. It is now clear that one way to minimize its two leading coefficients is to minimize

$$\|[t_{i-1},t_{i-1},t_i]\boldsymbol{s}_i\|^2 + \|[t_{i-1},t_{i-1},t_i,t_i]\boldsymbol{s}_i\|^2.$$

This idea is based on minimization of unwanted oscillations, introduced by polynomials of high degrees. But unfortunately it turns out that this approach leads to a complicated analysis. In order to keep things as simple as possible, the observation that

$$\|[t_{i-1},t_{i-1},t_i,t_i]\boldsymbol{s}_i\| \le \frac{1}{\Delta t_{i-1}}\left(\|[t_{i-1},t_{i-1},t_i]\boldsymbol{s}_i\| + \|[t_{i-1},t_i,t_i]\boldsymbol{s}_i\|\right)$$

suggests to minimize

$$\psi_i(\boldsymbol{\alpha}_i) := \|[t_{i-1},t_{i-1},t_i]\boldsymbol{s}_i\|^2 + \|[t_{i-1},t_i,t_i]\boldsymbol{s}_i\|^2, \tag{6}$$

instead. Indeed, if $\psi_i(\boldsymbol{\alpha}_i) = 0$, then

$$[t_{i-1},t_{i-1},t_i]\boldsymbol{s}_i = [t_{i-1},t_{i-1},t_i,t_i]\boldsymbol{s}_i = \boldsymbol{0},$$

and $\boldsymbol{s}_i$ in (5) reduces to a straight line. On the other hand, ψ_i can be viewed as a discrete approximation of φ_i. Namely,

$$[t_{i-1},t_{i-1},t_i]\boldsymbol{s}_i = \frac{1}{2}\boldsymbol{s}_i''(\xi_1), \quad [t_{i-1},t_i,t_i]\boldsymbol{s}_i = \frac{1}{2}\boldsymbol{s}_i''(\xi_2), \quad \xi_1,\xi_2 \in [t_{i-1},t_i],$$

which implies

$$\psi_i(\boldsymbol{\alpha}_i) = \frac{1}{2}\|\boldsymbol{s}_i''(\xi_3)\|^2, \quad \xi_3 \in [t_{i-1},t_i],$$

i.e., a zeroth order approximation of $2\varphi_i/\Delta t_{i-1}$. Thus, instead of minimizing φ_i, the minimization of ψ_i will be done.

An optimal choice of $\boldsymbol{\alpha}_i$ is stated in the following theorem.

Theorem 1 *The nonlinear functional ψ_i, $i = 1,2,\ldots,n$, has a unique global minimum in the interior of $\mathcal{D}_i$ iff*

$$\boldsymbol{\alpha}_i^* := \frac{1}{\Delta t_{i-1}}\left(\langle \boldsymbol{d}_{i-1}, \Delta\boldsymbol{T}_{i-1}\rangle, \langle \boldsymbol{d}_i, \Delta\boldsymbol{T}_{i-1}\rangle\right)^T > \boldsymbol{0}.$$

Furthermore,

$$\min_{\boldsymbol{\alpha}_i \in \mathcal{D}_i} \psi_i(\boldsymbol{\alpha}_i) = \frac{2 - c_{i,0}^2 - c_{i,1}^2}{(\Delta t_{i-1})^4}\,\|\Delta\boldsymbol{T}_{i-1}\|^2,$$

where

$$c_{i,k} = \cos\angle\left(\boldsymbol{d}_{i+k-1}, \Delta\boldsymbol{T}_{i-1}\right), \quad k = 0,1.$$

Proof Some basic properties of divided differences together with (2) simplify (6) to

$$\psi_i(\boldsymbol{\alpha}_i) = \frac{1}{(\Delta t_{i-1})^4}\left((\Delta t_{i-1})^2 \left(\alpha_{i,0}^2 + \alpha_{i,1}^2\right) - 2\,\Delta t_{i-1}\cdot \right.$$
$$\left. \langle \alpha_{i,0}\,\boldsymbol{d}_{i-1} + \alpha_{i,1}\,\boldsymbol{d}_i, \Delta \boldsymbol{T}_{i-1}\rangle + 2\,\|\Delta \boldsymbol{T}_{i-1}\|^2\right).$$

Minima of ψ_i are either on the boundary of $\mathcal{D}_i$ or they are obtained by taking partial derivatives of ψ_i. In the later case, a local minimum appears at $\boldsymbol{\alpha}_i^* := \left(\alpha_{i,0}^*, \alpha_{i,1}^*\right)^T$, where

$$\alpha_{i,k}^* = \frac{\langle \boldsymbol{d}_{i+k-1}, \Delta \boldsymbol{T}_{i-1}\rangle}{\Delta t_{i-1}}, \quad k = 0, 1,$$

which leads to

$$m := \psi_i(\boldsymbol{\alpha}_i^*) = \frac{2 - c_{i,0}^2 - c_{i,1}^2}{(\Delta t_{i-1})^4}\,\|\Delta \boldsymbol{T}_{i-1}\|^2.$$

It remains to prove that this is a global minimum as well. Take any $\boldsymbol{\alpha}_i = (\alpha_{i,0}, \alpha_{i,1})^T$ on the boundary of $\mathcal{D}_i$. Thus $\alpha_{i,k} = 0$ for at least one $k \in \{0, 1\}$. If $\alpha_{i,0} = \alpha_{i,1} = 0$ then $\psi_i(\boldsymbol{\alpha}_i) = 2\,\|\Delta \boldsymbol{T}_{i-1}\|^2/(\Delta t_{i-1})^4 \geq m$, and it remains to consider the case when only one of $\alpha_{i,k}$ is positive. Due to the symmetry, it is enough to study $\alpha_{i,0} > 0$ only. But in this case it is easy to check that the functional $\psi_i|_{\alpha_{i,1}=0}$ attains its global minimum at $\alpha_{i,0} = \langle \boldsymbol{d}_{i-1}, \Delta \boldsymbol{T}_{i-1}\rangle/\Delta t_{i-1}$ implying $\psi_i(\alpha_{i,0}, 0) = \left(2 - c_{i,0}^2\right)\,\|\Delta \boldsymbol{T}_{i-1}\|^2/(\Delta t_{i-1})^4 \geq m$. This concludes the proof of the theorem. □

Notice that the minimum can also be zero. In this case $c_{i,0} = c_{i,1} = 0$ and the cubic parametric spline segment $\boldsymbol{s}_i$ reduces to a straight line $\boldsymbol{s}_i(t) = \boldsymbol{T}_{i-1} + (t - t_{i-1})[t_{i-1}, t_i]\boldsymbol{s}_i$.

Corollary 1 *The conditions $\boldsymbol{\alpha}_i^* > \boldsymbol{0}$, $i = 1, 2, \ldots, n$, have a simple geometric interpretation, i.e., $\angle\left(\boldsymbol{d}_{i+k-1}, \Delta \boldsymbol{T}_{i-1}\right) \in [0, \frac{\pi}{2})$, $k = 0, 1$.*

Now suppose that the assumptions of Theorem 1 are satisfied. Then an important question arises whether the resulting cubic spline segment $\boldsymbol{s}_i$ is regular on $[t_{i-1}, t_i]$, $i = 1, 2, \ldots, n$. The answer is confirmative, even more, $\boldsymbol{s}_i$ has no cusps, loops or folds and is independent of the parameterization (1) as stated in the following theorem.

Theorem 2 *Let the assumptions of Theorem 1 be satisfied and let $\boldsymbol{s}_i$ be the resulting Hermite geometric interpolant defined by* (2)*. Then the spline segment $\boldsymbol{s}_i$ is regular, loop-, cusp-, fold-free and parameterization independent on $[t_{i-1}, t_i]$, $i = 1, 2, \ldots, n$.*

Proof By generalizing the ideas for the planar case in [8], it can be shown that the claims of the theorem hold. The proof will be omitted. □

One of the possible heuristic approaches on how to automatically choose proper tangent directions, is addressed in the following remark.

Remark 1 By considering the approach for the planar case, described in [8] on triples of consecutive data points, an admissible set of tangent directions can be constructed automatically. The algorithm is as follows. Consider Fig. 1. First, take vectors $\boldsymbol{T}_{i-1}\boldsymbol{T}_i$ and $\boldsymbol{T}_{i+1}\boldsymbol{T}_i$, normalize them and set them at the point $\boldsymbol{T}_i$. Let us denote the vectors by $\boldsymbol{u}_i$ and $\boldsymbol{v}_i$, respectively. Let a normalized vector $1/2 \cdot (\boldsymbol{u}_i + \boldsymbol{v}_i)$ be denoted by $\boldsymbol{s}_i$. Let z be -1, if the third component of the cross product $\Delta\boldsymbol{T}_{i-1} \times \Delta\boldsymbol{T}_i$ is negative, and 1, otherwise. Now rotate the vector $\boldsymbol{s}_i$ around $\boldsymbol{T}_i$ by an angle of $z \cdot \pi/2$ in the positive direction. Thus constructed vector $\boldsymbol{d}_i$ is an admissible tangent direction (in Fig. 1 the admissible area in the plane, defined by $\boldsymbol{T}_{i-1}, \boldsymbol{T}_i, \boldsymbol{T}_{i+1}$ is colored in gray). With so constructed additional data, a unique interpolating spline can be constructed by Theorem 1 and (2).

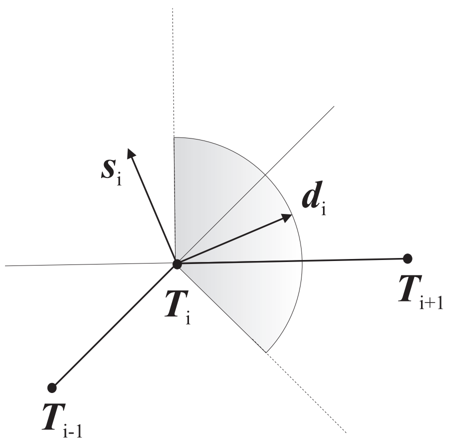

Fig. 1 A local construction of a tangent direction $\boldsymbol{d}_i$ at $\boldsymbol{T}_i$.

The main result of this paper can be generalized to $\mathbb{R}^d, d \geq 3$.

Remark 2 Note that Theorem 1 can be straightforwardly generalized to interpolation of data points in the space $\mathbb{R}^d$ for any $d \geq 3$. The tangent directions should be constructed in such a way, that the conditions of Corollary 1 are satisfied. Note that a higher dimension d brings additional shape parameters. This can be exploited for fine tuning the shape of the interpolant.

4 Examples

Let us conclude the paper by numerical examples. First consider Fig. 2. A cubic G^1 Hermite interpolant (solid curve), constructed by our method, closely resembles the C^2 cubic interpolating spline (dotted curve). In our scheme, based on Theorem 1, instead of solving a global system of equations, we had to solve a sequence of small systems. This can be done much more efficiently than in the C^2 case, where solving of a large global system can not be avoided. Here, the tangent directions were chosen by using the approach, described in Remark 1. Of course, any other choice of admissible tangent directions would result in an appropriate curve. Our approach in some sense minimizes the deviation of the interpolatory curve from the data polygon by considering osculating planes at the data points.

In Fig. 2 there is also a dashed curve which represents the well-known Akima interpolant (see [1]). This linear scheme also generates a G^1 curve based on data points only and it can be clearly seen that our method gives comparable results.

In Fig. 3 it can be seen that our interpolant is practically indistinguishable from the C^2 cubic interpolant, if the data are sampled from a spiral $(\cos t, \sin t, t)$ at equidistant parameters $t_i = 0, 1, \ldots, 20$.

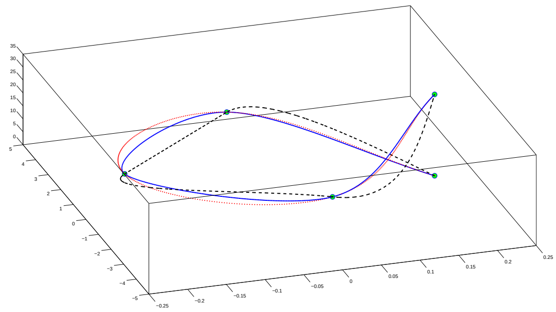

Fig. 2 Hermite G^1 interpolating spline (solid), C^2 cubic spline interpolant (dotted) and Akima interpolant (dashed) of a "space" epitrochoid given by $((R+r)\cos t - d\cos((R+r)t/r), (R+r)\sin t - d\sin((R+r)t/r), t)$ with $R = 1.2$, $r = 1$ and $d = 2$ at the parameters $t_i = 0, 7.85, 15.71, 23.56, 31.42$.

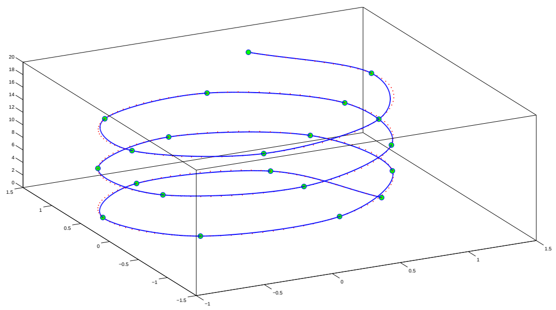

Fig. 3 Hermite G^1 interpolating spline (solid) and the C^2 cubic spline interpolant (dotted) for the data, sampled from a spiral $(\cos t, \sin t, t)$ at parameters $t_i = 0, 1, \ldots, 20$.

References

1. Akima, H.: A new method of interpolation and smooth curve fitting based on local procedures. J. of the ACM, 17(4):589–602 (1970)
2. de Boor, C.: A practical guide to splines. Volume 27 of Applied Mathematical Sciences. Springer-Verlag, New York (2001)
3. de Boor, C., Höllig, K., Sabin, M.: High accuracy geometric Hermite interpolation. Comput. Aided Geom. Design, 4(4):269–278 (1987)
4. Dyn, N., Levin, D.: Subdivision schemes in geometric modelling. Acta Numer. 11: 73–144 (2002)
5. Farin, G.: Curves and surfaces for computer-aided geometric design. Academic Press Inc., San Diego, CA (1997)
6. Höllig, K., Koch, J.: Geometric Hermite interpolation with maximal order and smoothness. Comput. Aided Geom. Design, 13(8):681–695 (1996)
7. Jaklič, G., Kozak, J., Krajnc, M., Žagar, E.: On geometric interpolation by planar parametric polynomial curves, Math. Comp. 76:1981–1993 (2007)
8. Jaklič, G., Žagar, E.: Planar cubic G^1 interpolatory splines with small strain energy. Submitted.
9. Kozak, J., Krajnc, M.: Geometric interpolation by planar cubic G^1 splines. BIT, 47(3):547–563 (2007)
10. Wallner, J.: Note on curve and surface energies. Comput. Aided Geom. Design, 24:494–498 (2007)
11. Yong, J.-H., Cheng, F.: Geometric Hermite curves with minimum strain energy. Comput. Aided Design **21**, 281–301 (2004)